Brief Communication

Transient uterine hypercontractility causes oxidative stress in the fetal brain and sex-dependent mitochondrial and behavioral abnormalities in adolescent male rat offspring

Arvind Palanisamy[1], Tusar Giri[1], Jia Jiang[1], Annie Bice[2], James D. Quirk[2], Sara B. Conyers[3], Susan E. Maloney[3], Adam Q. Bauer[2], Joel R. Garbow[2], David F. Wozniak[3]

[1]Department of Anesthesiology, Washington University School of Medicine, St. Louis, MO
[2]Mallinckrodt Institute of Radiology, Washington University School of Medicine, St. Louis, MO
[3]Department of Psychiatry, Washington University School of Medicine, St. Louis, MO

Abstract: The neurodevelopmental impact of transient ischemic-hypoxemic insult during labor is poorly understood. Here, using an oxytocin-induced uterine hypercontractility paradigm, we confirm transient uteroplacental compromise, increased oxidative stress in the fetal brain, and enduring social behavioral impairment in male offspring with persistent upregulation of mitochondrial proteins in the anterior cingulate cortex. Our findings, therefore, indicate persistent mitochondrial dysfunction as a possible mechanistic link between intrauterine asphyxia and neurodevelopmental disorders.

Epidemiological studies reveal a link between obstetric complications and neurodevelopmental disorders (NDD),[1-5] but the underlying biological mechanisms remain largely unexplored. Particularly, the long-term neurodevelopmental impact of transient and less severe hypoxemic insults, which are more common during labor and delivery,[6,7] is poorly understood. Here, we show that transient ischemia-hypoxemia, induced by oxytocin (OXT) induced uterine hypercontractility, causes significant oxidative stress in the fetal brain, enduring brain-region specific dysfunction of the mitochondrial electron transport chain complex, and subtle neurobehavioral abnormalities in the adolescent offspring.

We first quantified the effect of OXT-induced uterine hypercontractility on placental perfusion in term pregnant Sprague Dawley rats (E21) with dynamic contrast-enhanced MRI (**Fig. 1A**).[8] Placental uptake of Dotarem® contrast was approximately 50% slower post-OXT, indicating a significant decrease in uteroplacental blood flow. This was accompanied by a significant decrease in placental R2* reflecting the absence of deoxygenated blood presumably due to profound placental squeeze (Suppl Fig. 1).Consequently, we determined the impact of transient placental ischemia-hypoxemia on the developing brain by assaying for lactate and oxidative stress markers. 4 h after OXT fetal brain lactate and oxidative stress markers (4-hydroxynonenal, protein carbonyl) were significantly higher, and the antioxidant capacity (GSSG/GSH ratio) lower, confirming increased oxidative stress after transient placental hypoxemia-ischemia (**Fig. 1B**). Next, we assessed the effect of ischemia-hypoxemia on gene expression changes in the fetal cerebral cortex using RNA-seq. 24 h after OXT, only 3 genes (*mt-nd2*, *mt-nd4*, *mt-atp6*), all related to the mitochondrial electron transport chain (ETC), were found to be significantly differentially expressed (**Fig. 1C**). Notably, there was no treatment-related difference in the expression of the oxytocin receptor (oxtr) gene (Suppl Fig. 2). This broadly suggested that the main effect of OXT-induced hypercontractility was oxidative stress and possible mitochondrial dysfunction in the fetal brain.

Considering these effects, we predicted long-term functional consequences for the fetus and therefore, evaluated OXT- and saline (SAL)-exposed offspring on several behavioral tests between PND 28-45. Social investigation time of a novel conspecific was significantly decreased in male, but not female, OXT-exposed offspring relative to male SAL-exposed offspring. In the observational fear learning (OFL) test, OXT offspring exhibited significantly increased freezing levels during the last 2 min of the training period despite comparable levels found between groups during baseline and during the first two minutes of training, but no sex effects were observed (**Fig. 2A**). No differences between groups were observed for the OFL contextual fear test conducted 24 h later (Suppl Fig. 2). The differences in freezing levels during training were not likely due to differences in ambulatory activity between the groups since they performed similarly on this variable during a 1-h open-field test (Suppl Fig. 3). These results suggest a heightened empathy-like fear response in the OXT-exposed offspring when observing a conspecific during brief distress.

Because of sex-dependent effects in some behavioral tasks, we investigated gene expression changes related to mitochondrial function and oxidative stress at an earlier timepoint — 1 h after OXT-induced uterine hypercontractility — in both male and female offspring. Specifically, we performed planned comparisons of treatment-related differences in the expression of select target genes related to ETC/oxidative stress, anti-oxidant defense, and hypoxia/apoptosis pathways using prevalidated Taqman®-specific probes. Multiple genes were differentially expressed in a sex-dependent manner; overall, there was an increased expression of genes related to ETC/oxidative stress (*mt-nd4, mt-nd5, mt-atp8*), anti-oxidant defense (*sod2, cygb*), and hypoxia/apoptosis (*casp8, hif1a*) pathways in treated males vs. females (**Fig. 2B**). We then selectively quantified changes in proteins emblematic of these pathways with immunoblots (HIF-1alpha from nuclear extracts at 1 h, cleaved caspase-3 [CC3] from whole cortical lysates at 18 h, OXPHOS proteins in the mitochondrial fraction isolated from the anterior cingulate cortex at PND 28). There were no treatment or sex-related differences in either HIF-1alpha or CC3 (Suppl figs. 4 & 5, respectively), suggesting that the related gene expression changes were probably transient. However, OXPHOS proteins related to mitochondrial ETC complex I, III, and IV were selectively higher in the anterior cingulate cortex of PND 28 male OXT-exposed offspring (**Fig. 2C**). Given the importance of the anterior cingulate cortex in both social and empathy-related behavior,[9-11] we speculate that the sex differences in behavior may be partly related to altered expression of proteins related to mitochondrial ETC in this region. To determine if there were consequences for functional connectivity (FC), we performed FC analysis with optical intrinsic signaling (OIS) in a separate cohort of male offspring (Suppl fig. 6).[12] Among the brain regions that could be meaningfully studied, we detected significant differences in FC only in the somatosensory cortex of OXT-exposed male pups (**Fig. 2D**).

In conclusion, transient intrauterine ischemia-hypoxemia was associated with male-specific differences in social behavior, differential expression of selective oxidative stress genes in the developing cortex, and enduring upregulation of mitochondrial ETC proteins in the anterior cingulate cortex. Collectively, our findings support the possibility of persistent mitochondrial dysfunction as a mechanistic link between transient intrauterine asphyxia and NDD and identify the anterior cingulate cortex as a brain region of susceptibility and significance.

Methods

1. Animals and Drugs: All experiments reported here were approved by the Institutional Animal Care and Use Committee at Washington University in St. Louis (#20170010) and comply with the ARRIVE guidelines. Timed pregnant Sprague Dawley (SD) rats (Charles River Laboratories, Wilmington, MA) were used for all experiments. Oxytocin (OXT; Selleck Chemicals, Houston, TX) was prepared as a 1mg/mL solution in sterile normal saline. We developed a rapid method to identify the sex of the pups using visual inspection of the anogenital distance at E21. Another experimenter cross-checked and verified the sex by performing a mini-laparotomy to identify the presence (male) or absence (female) of testes and seminal vesicles.

2. Placental imaging: SD dams at E21 (n=3) were anesthetized with isoflurane in 100% oxygen and imaged on an Agilent (Santa Clara, CA) 4.7T DirectDrive MRI system using a 7.2 cm inner diameter quadrature RF coil. Anatomic scans were initially acquired across the entire abdomen using a respiratory-gated T2-weighted 2D multi-slice fast spin echo sequence (FSEMS; 0.5 x 1 x 1 mm^3 resolution, zero-padded to 0.5 x 0.5 x 1 mm^3, TR/TE = 2000/48 ms, echo train length = 4, 4 averages, respiratory gated, imaging time approximately 6 min depending upon respiration rate). Placental blood flow was measured by dynamic contrast enhanced (DCE) MRI with a tail vein injection of Dotarem® (Guerbet, Princeton, NJ, 0.2 mmol/kg). The rats were then injected with 100 μg/kg of OXT through a 22G tail vein catheter to induce uterine contraction. Following the cessation of gross abdominal motion, typically around 30 min as assessed by non-gated low-resolution scouts, the anatomic scan was re-acquired to account for placental displacement during the contraction period and the DCE measurement was repeated with a repeat dose of the same contrast agent. Placental perfusion was quantified as the initial area under the curve (IAUC) of the DCE time-intensity for each placental voxel using the DCE@urLAB package.[13] Each rat placenta was manually segmented from pre- and post-OXT anatomical images using customized MATLAB routines and interpolated onto the IAUC maps. As the DCE protocol involved two injections of contrast agent separated by approximately 50 min, the time under anesthesia and the presence of residual contrast agent from the first injection could potentially distort the post-OXT DCE results. To examine the size of these effects, we repeated the DCE protocol on a dam where we injected the same volume of saline instead of OXT. Under these conditions, the IAUC post-saline injection across placentas was within 2% of the pre-injection values, indicating that OXT was responsible for the perfusion changes observed in Figure 1A.

3. Lactate assay: To determine if OXT-induced uterine contractions induce hypoxemia in the fetal brain, we assayed for fetal brain lactate 4 h after 100 μg/kg i.v OXT or saline in timed pregnant E21 Sprague Dawley (SD) dams (n = 8 each). Briefly, whole male and female fetal brains were homogenized on ice and deproteinized with 10 kDa molecular weight cut-off spin filter to remove lactate dehydrogenase. Protein concentrations were determined using BCA Protein Assay Kit (ThermoFisher Scientific), followed by lactate assay (Lactate Colorimetric Assay Kit II; Sigma-Aldrich) according to manufacturer's instructions. Results calculated from standard curve are expressed as nmoL/mg brain protein. Outliers were detected and eliminated using ROUT (robust regression and outlier analysis) with Q set to 10%. Normality of residuals was checked with D'Agostino-Pearson omnibus test followed by 2-way ANOVA and Sidak's

multiple comparisons test to assess for significant sex-dependent differences in the treated group. Data presented as mean ± SEM.

4. Oxidative stress assays: To determine if OXT causes oxidative stress in the fetal brain, we assayed male and female fetal brains for 4-hydroxynonenal (4-HNE, a byproduct of lipid peroxidation), protein carbonyl, and the antioxidant GSSG/GSH in the same E21 dams used for the lactate assay. Briefly, whole fetal brains were homogenized in PBS buffer on ice. Protein concentrations were determined using BCA Protein Assay Kit (Thermo Scientific), followed by 4-HNE assay (OxiSelect™ HNE Adduct Competitive ELISA Kit;), protein carbonyl (OxiSelect™ Protein Carbonyl ELISA kit), and total glutathione assay (OxiSelect™ GSSG/GSH Assay Kit) according to manufacturer's instructions. All assays were supplied by Cell Biolabs, Inc, San Diego, CA. Results calculated from the standard curve are expressed as mcg/mg of brain protein. Outliers were detected and eliminated using ROUT (robust regression and outlier analysis) with Q set to 10%. Normality of residuals was checked with D'Agostino-Pearson omnibus test followed by 2-way ANOVA and Sidak's multiple comparisons test to assess for significant sex-dependent differences in the treated group. Data presented as mean ± SEM.

5. RNA-sequencing: E21 timed pregnant SD rats were treated with either 100 μg/kg OXT or saline through a 22G tail vein catheter (n = 5 each). 24 h later, fetal brains were harvested under isoflurane anesthesia. Total RNA was extracted the right cerebral cortex using RNAeasy kit (Qiagen). Only RNA with RIN > 9.5 were used for RNA-seq. RNA-seq reads were aligned to the Ensembl top-level assembly with STAR version 2.0.4b. Gene counts were derived from the number of uniquely aligned unambiguous reads by Subread: featureCount version 1.4.5. Transcript counts were produced by Sailfish version 0.6.3. Sequencing performance was assessed for total number of aligned reads, total number of uniquely aligned reads, genes and transcripts detected, ribosomal fraction known junction saturation and read distribution over known gene models with RSeQC version 2.3.All gene-level and transcript counts were then imported into the R/Bioconductor package EdgeR and TMM normalization size factors were calculated to adjust for samples for differences in library size. Genes or transcripts not expressed in any sample were excluded from further analysis. The TMM size factors and the matrix of counts were then imported into R/Bioconductor package Limma and weighted likelihoods based on the observed mean-variance relationship of every gene/transcript and sample were then calculated for all samples with the voomWithQualityWeights function. Performance of the samples was assessed with a spearman correlation matrix and multi-dimensional scaling plots. Gene/transcript performance was assessed with plots of residual standard deviation of every gene to their average log-count with a robustly fitted trend line of the residuals. Generalized linear models were then created to test for gene/transcript level differential expression. Differentially expressed genes and transcripts were then filtered for FDR adjusted p-values ≤ 0.2.

6. Behavioral experiments: Male and female offspring of E21 SD dams (n = 9 each) treated with OXT (100 μg/kg) or saline (OXY or SAL rats, respectively) were subjected to behavioral testing. There were no differences in litter size, sex ratio, or survival of the offspring from both treatment groups. Pups were weaned on P21 and subsequently evaluated on a battery of behavioral tests from postnatal day (PND) 26-45 in the following order: 1) 1h open field; 2) social approach; 3) elevated plus maze; and 4) observational fear learning[14] The OXT and SAL rats were tested in two cohorts (n = 6 and 3 dams each, respectively) for which identical

behavioral protocols were used. A total of 12 male and female offspring from the OXT and SAL group were tested. Details of all behavioral experimental procedures are included in the supplementary file and described previously.[15] Data were typically analyzed using repeated measures ANOVA models to evaluate effects of treatment, sex, and time-related variables. Data are presented as mean ± SEM. The critical alpha value for all analyses was $p < 0.05$, unless otherwise stated. See Supplemental File for more details.

7. Taqman qPCR: Male and female fetal brains exposed to either 100 μg/kg OXT (n = 8) or saline (n = 8) *in utero* were harvested and immediately stored at -80 °C. RNA was extracted using RNeasy plus mini kit (Qiagen), converted to cDNA using SuperScript® IV VILO™ master mix kit (Invitrogen), and 25 ng of the template cDNA was then combined with a ready-to-use TaqMan Fast Advanced qPCR Master Mix (Thermo Fisher Scientific, Waltham, MA) for experiments in a pathway-specific custom TaqMan array (Custom TaqMan® Array Fast Plate 96, Life Technologies, Carlsbad, CA). Expression levels of 28 genes relevant to three specific pathways mitochondrial electron transport chain (ETC) complexes (*mt-cyb, mt-nd1, mt-nd2, mt-nd4, mt-nd5, mt-atp6, mt-atp8, mt-co1, mt-co3, nox4, nos2)*, oxidative stress and anti-oxidant defense (*cat, gpx1, gpx2, gsr, prdx1, sod1, sod2, srxn1, nqo1, mt3, cygb*), and hypoxia, stress and toxicity (*bax, bcl2l1, casp8, hif1a, nfkb1*) were assayed in triplicate along with four endogenous housekeeping control genes (*18S rRNA, gapdh, pgk1,* and *actb*). Thermal cycling was performed in 7500 Fast Real-Time PCR System (Applied Biosystems®, Foster City, CA) and the threshold cycle (Ct) values for all genes were calculated using proprietary software. We tested the experimental stability of all 4 endogenous reference genes using the geNorm algorithm and determined *pgk1* to be the most stable reference gene. Relative mRNA expression, normalized to *pgk1*, was calculated using the $2^{-\Delta\Delta CT}$ method with sex-matched control samples as reference. Outliers were detected and eliminated using ROUT (robust regression and outlier analysis) with Q set to 10%. Normality of residuals was checked with D'Agostino-Pearson omnibus test followed by 2-way ANOVA and Sidak's multiple comparisons test to assess for significant sex-dependent differences in the treated group. Data with non-normal residuals (*mt-atp6, mt-co1, nox4, cat, gsr, prdx1, sod2, bcl2l1, hif1a*) were Box-Cox transformed prior to statistical testing. Data presented as mean ± SEM.

8. Western blotting: Fetal cortical lysates (≈100 mg) were extracted using RIPA buffer (50 mM Tris HCl pH 7.5, 150 mM NaCl, 2 mM EDTA, 1% NP40, 0.1% SDS) with protease and phosphatase inhibitor cocktail (ThermoFisher Scientific Inc). Mitochondrial and nuclear fractions from the fetal cortex were separately prepared using appropriate kits (mitochondrial isolation kit, catalog # 89801 and subcellular protein fractionation kit, catalog # 87790, ThermoFisher Scientific Inc) following manufacturer's instructions. Approximately 30 μg of protein was subjected to gel electrophoresis and transferred to membrane using Bolt western blot reagents from ThermoFisher Scientific Inc (bolt 4-12% Bis Tris gel, catalog # NW04125; bolt sample reducing agent, catalog # B0009; bolt LDS sample buffer, catalog # B0007; iBlot2 dry blotting system). Membranes were blocked with TBST buffer (catalog # S1012, EZ Bioresearch), containing 5% milk for 1 hour at room temperature on a shaker. Following a brief wash with TBST buffer, the membranes were immunoblotted overnight at 4 °C on a shaker with antibodies against hif1a (Catalog # 14179, Cell Signaling Technology), cleaved caspase 3 (Asp-175) (Catalog # 9661, Cell Signaling Technology), OXPHOS rodent ab cocktail (ab110413) (Catalog # MS604300, Abcam Inc). Beta-actin (Catalog # MA5-11869,

ThermoFisher Scientific Inc), VDAC1 (Catalog # ab 15895, Abcam Inc), and histone H3 (Catalog # 9715S, Cell Signaling Technology) were used for normalization. For OXPHOS experiments, rat heart mitochondria were used as positive control. All the primary antibodies were used at a dilution of 1:1000. HRP-conjugated secondary antibodies (anti-Rab IgG, catalog #7074 and anti-mouse IgG, catalog #7076, Cell Signaling Technology) were used at a dilution of 1:1000 for 1 hour at room temperature on a shaker. Immunoblots were incubated with Western ECL substrate (catalog # 1705060, Bio-Rad Inc) for 5 minutes at room temperature, followed by exposure to film inside a cassette in dark room, and developed using Konica Minolta Inc, Film Processor (catalog # SRX-101A). Western blot images were processed with ImageJ for densitometric quantification.

9. Functional connectivity analysis: Functional connectivity of the brain of OXT-exposed male offspring was assessed at P23 using a reflectance-mode functional connectivity optical intrinsic signal (fcOIS) imaging system.[12] The fcOIS system images the brain through the intact skull and records spontaneous fluctuations in oxy- and deoxyhemoglobin. Through neurovascular coupling, these fluctuations represent spatio-temporal variations in neural activity, similar to human BOLD-fMRI. Quantitative differences in homotopic fc in 7 brain regions were compared as shown in Fig 2d. Significant differences in fc was observed only for the somatosensory cortex. Data were analyzed with student's t-test and presented as mean ± SEM.

Figure 1

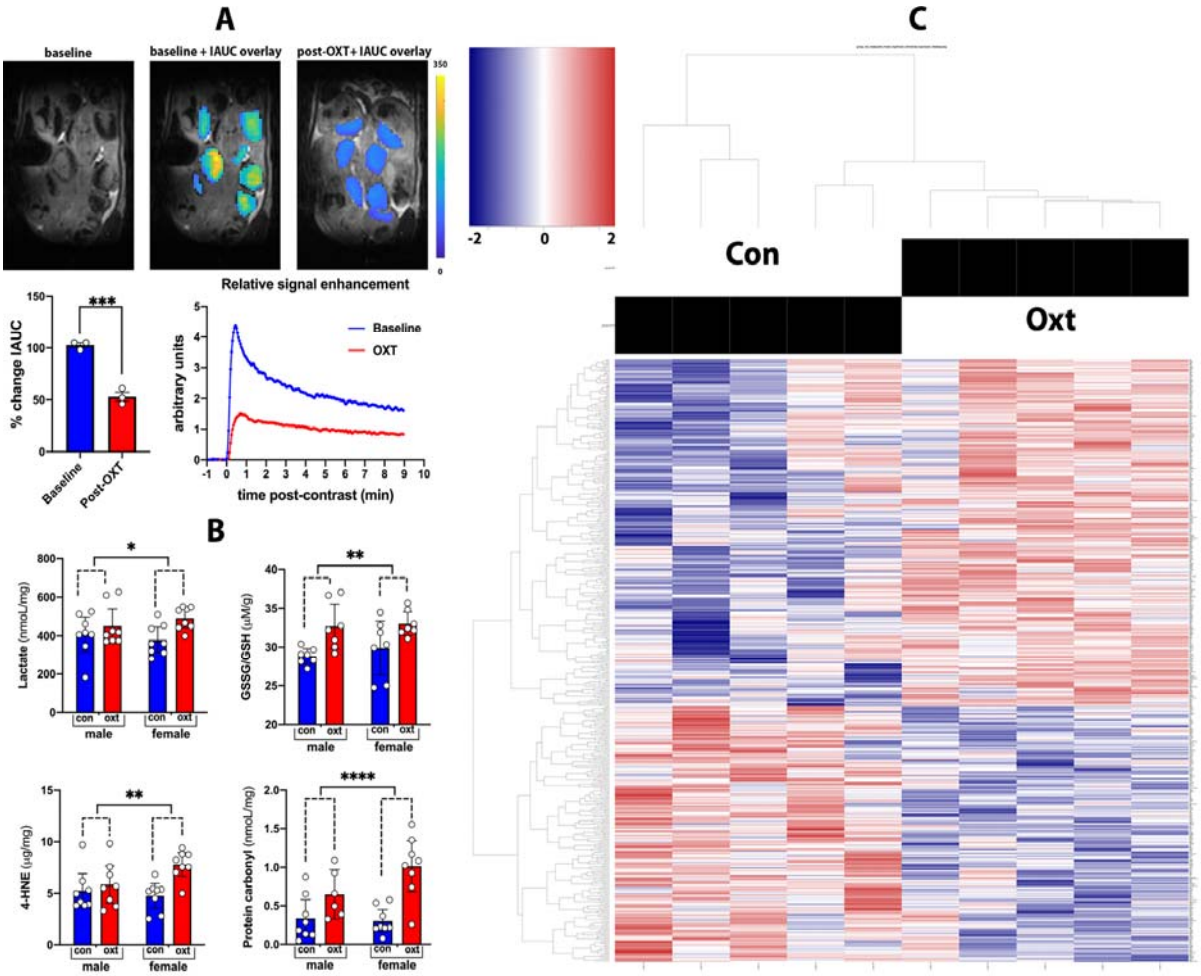

Figure 1. A) Placental perfusion is severely impaired after OXT-induced uterine hypercontractility. Top: middle and right panels show the initial area under the curve (IAUC) from the baseline and post-OXT DCE experiments overlaid onto the corresponding anatomical T2w images from one slice. Bottom: left panel shows a significant decrease in IAUC averaged across all placentas after OXT (*******p=0.0006), and right panel shows a significant decrease in placental relative signal enhancement after Dotarem® injection. **B) Transient OXT-induced uterine hypercontractility causes oxidative stress in the fetal brain.** *In utero* exposure to OXT-induced uterine hypercontractility was associated with an increase, compared to saline-exposed pups, in fetal brain lactate (*****p = 0.02), oxidized GSSG/GSH (******p=0.001), 4-hydroxynonenal (******p=0.007), and protein carbonyl (********p<0.0001) at 4 h suggestive for oxidative stress. Data analyzed with 2-way ANOVA and presented as mean ± SEM. *p<0.05, **p<0.01, ***p<0.001, ****p<0.0001. **C) OXT-induced uterine hypercontractility selectively affects the differential expression of mitochondrial electron transport chain (ETC) genes.** RNA-seq heat map showing differential expression of cortical genes in E21 offspring 24 h after OXT or saline treatment (n=5 dams each). Of the 584 genes that were differentially expressed,

only 3 genes (*mt-nd2*, *mt-nd4*, *mt-atp6*), all related to the mitochondrial ETC, passed the FDR adjusted p-value cutoff of ≤ 0.2.

Figure 2

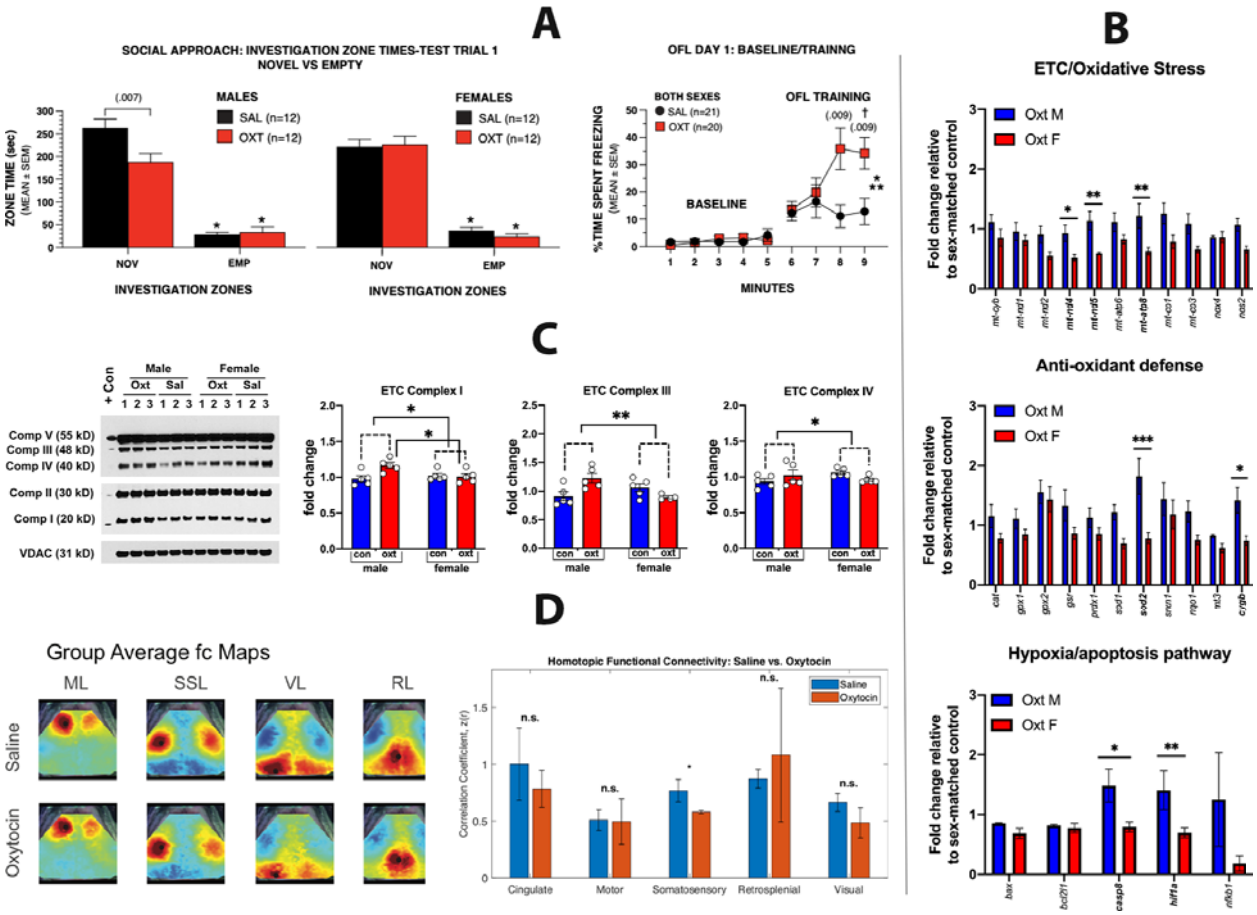

Figure 2. A) OXT-induced uterine hypercontractility is associated with male-specific decrease in social investigation and an increase in empathic-like fear. Left panel: Male OXT-offspring rats spent significantly less time investigating a novel rat compared to that exhibited by male SAL-offspring rats (p=0.007; treatment effect, p=0.016; treatment x sex interaction, p=0.038). No differences were observed between female-offspring groups. Right panel: OXT offspring showed significantly increased freezing levels in the OFL test during the last 2 min of training (min 8 & 9, p=0.009 for each, significant after Bonferroni correction, p<0.0125)), suggesting an enhanced empathy-like response (treatment effect, *p=0.04; treatment x min interaction, **p=0.003). Also, the OXT offspring showed a significant increase in freezing levels from the first minute of training to the last minute (min 6 vs min 9: †p=0.007), while the SAL offspring did not. **B) OXT-induced hypercontractility causes sex-dependent gene expression changes in the E21 fetal cerebral cortex.** Multiple genes were differentially expressed in a sex-dependent manner after OXT-induced hypercontractility. Overall, there was an increased expression of genes related to ETC/oxidative stress (*mt-nd4*, *mt-nd5*, *mt-atp8*), anti-oxidant defense (*sod2*, *cygb*), and hypoxia/apoptosis (*casp8, hif1a*) pathways in treated males vs. females. *p<0.05, **p<0.01, and ***p<0.001. **C) OXT-induced hypercontractility causes enduring upregulation of OXPHOS proteins in the anterior cingulate cortex of male P28**

offspring. Left: Representative immunoblots of anterior cingulate cortex homogenates from P28 offspring showing increased expression of proteins related to the mitochondrial electron transport chain (OXPHOS) in males. Scatter plots show a significant increase in complex I (*p=0.02 for treatment x sex interaction [F (1, 16) = 6.5] and *p=0.04 for treatment [F (1, 16)= 5.0]), complex III (**p=0.004 for treatment x sex interaction [F (1, 15)]=12.0]), and complex IV (*p=0.04 for treatment x sex interaction, F (1, 16)=4.6) in OXT-exposed male, but not female, offspring. Normalization was done with mitochondrial VDAC1 protein. **D) Functional connectivity (fc) analysis in adolescent male offspring reveal abnormalities in the somatosensory cortex.** Left: FC maps in 4 representative brain regions from the left cortex (motor – ML, somatosensory – SSL, visual – VL, retrosplenial – RL) in P23 male rat offspring exposed to OXT-induced hypercontractility (n = 4) or saline (n = 3) *in utero*. Red pixels denote high positive functional connectivity with seeded region. Right: Quantitative comparisons of regional homotopic FC reveal significant group differences in the somatosensory cortex; *p< 0.05.

References

1. Kolevzon A, Gross R, Reichenberg A. Prenatal and perinatal risk factors for autism: a review and integration of findings. *Arch Pediatr Adolesc Med.* 2007;161(4):326-333.
2. Glasson EJ, Bower C, Petterson B, de Klerk N, Chaney G, Hallmayer JF. Perinatal factors and the development of autism: a population study. *Archives of general psychiatry.* 2004;61(6):618-627.
3. Dalman C, Thomas HV, David AS, Gentz J, Lewis G, Allebeck P. Signs of asphyxia at birth and risk of schizophrenia. Population-based case-control study. *Br J Psychiatry.* 2001;179:403-408.
4. Cannon M, Jones PB, Murray RM. Obstetric complications and schizophrenia: historical and meta-analytic review. *Am J Psychiatry.* 2002;159(7):1080-1092.
5. Modabbernia A, Mollon J, Boffetta P, Reichenberg A. Impaired Gas Exchange at Birth and Risk of Intellectual Disability and Autism: A Meta-analysis. *J Autism Dev Disord.* 2016;46(5):1847-1859.
6. Heuser CC, Knight S, Esplin MS, et al. Tachysystole in term labor: incidence, risk factors, outcomes, and effect on fetal heart tracings. *American journal of obstetrics and gynecology.* 2013;209(1):32 e31-36.
7. Kunz MK, Loftus RJ, Nichols AA. Incidence of uterine tachysystole in women induced with oxytocin. *J Obstet Gynecol Neonatal Nurs.* 2013;42(1):12-18.
8. Tomlinson TM, Garbow JR, Anderson JR, Engelbach JA, Nelson DM, Sadovsky Y. Magnetic resonance imaging of hypoxic injury to the murine placenta. *Am J Physiol Regul Integr Comp Physiol.* 2010;298(2):R312-319.
9. Apps MA, Rushworth MF, Chang SW. The Anterior Cingulate Gyrus and Social Cognition: Tracking the Motivation of Others. *Neuron.* 2016;90(4):692-707.
10. Hadland KA, Rushworth MF, Gaffan D, Passingham RE. The effect of cingulate lesions on social behaviour and emotion. *Neuropsychologia.* 2003;41(8):919-931.
11. Carrillo M, Han Y, Migliorati F, Liu M, Gazzola V, Keysers C. Emotional Mirror Neurons in the Rat's Anterior Cingulate Cortex. *Curr Biol.* 2019;29(8):1301-1312 e1306.
12. Bauer AQ, Kraft AW, Wright PW, Snyder AZ, Lee JM, Culver JP. Optical imaging of disrupted functional connectivity following ischemic stroke in mice. *Neuroimage.* 2014;99:388-401.
13. Ortuno JE, Ledesma-Carbayo MJ, Simoes RV, Candiota AP, Arus C, Santos A. DCE@urLAB: a dynamic contrast-enhanced MRI pharmacokinetic analysis tool for preclinical data. *BMC Bioinformatics.* 2013;14:316.
14. Kim A, Keum S, Shin HS. Observational fear behavior in rodents as a model for empathy. *Genes Brain Behav.* 2019;18(1):e12521.
15. Maloney SE, Yuede CM, Creeley CE, et al. Repeated neonatal isoflurane exposures in the mouse induce apoptotic degenerative changes in the brain and relatively mild long-term behavioral deficits. *Sci Rep.* 2019;9(1):2779.